AIP | Applied Physics Letters

Carrier dynamics and conductivity of SnO2 nanowires investigated by time-resolved terahertz spectroscopy

Demetra Tsokkou, Andreas Othonos, and Matthew Zervos

Citation: Appl. Phys. Lett. **100**, 133101 (2012); doi: 10.1063/1.3698097

View online: http://dx.doi.org/10.1063/1.3698097

View Table of Contents: http://apl.aip.org/resource/1/APPLAB/v100/i13

Published by the American Institute of Physics.

Carrier dynamics and conductivity of SnO_2 nanowires investigated by time-resolved terahertz spectroscopy

Demetra Tsokkou,[1] Andreas Othonos,[1,a)] and Matthew Zervos[2]
[1]*Department of Physics, Research Center of Ultrafast Science, University of Cyprus, P.O. Box 20537, Nicosia 1678, Cyprus*
[2]*Department of Mechanical Engineering, Nanostructured Materials and Devices Laboratory, University of Cyprus, P.O. Box 20537, Nicosia 1678, Cyprus*

(Received 6 February 2012; accepted 7 March 2012; published online 26 March 2012)

THz spectroscopy has been applied to investigate the photo-induced and intrinsic conductivity in SnO_2 nanowires using the Drude-Smith model. The refractive index of the nanowires was found to decrease from 2.4 to 2.1 with increasing THz frequency and the dc mobility of the non-excited nanowires was determined to be 72 ± 10 cm^2/Vs. Measurements reveal that scattering times are carrier density dependent, while a strong suppression of long transport is evident. Intensity-dependent measurements provided an estimate of the Auger coefficient found to be $\gamma = (7.2 \pm 2.0) \times 10^{-31}$ cm^6/s.
 [http://dx.doi.org/10.1063/1.3698097]

Tin oxide (SnO_2) is considered an important n-type wide-bandgap semiconductor which has received a great deal of attention over the past few years mainly due to its high transparency in the visible part of the spectrum and sensitivity to certain gasses which make it technologically important for the fabrication of optoelectronic devices[1–3] and sensors.[4] Furthermore, in recent years, the field of semiconducting metal oxides has benefited a great deal from the development of one-dimensional nanostructures such as nanowires (NWs) and nanorods (NRs) due to their interesting properties arising from their small size and high surface-to-volume ratio.[5] In view of this there has been growing interest in the synthesis of SnO_2 NWs, the study of their fundamental electronic and optoelectronic properties and finally device applications.[6–8] Time domain THz spectroscopy (TDTS) and time resolved THz spectroscopy (TRTS) have been recently used to provide insight into the physical properties of semiconductor nanostructured materials, such as nanoparticles[9,10] and nanowires.[11,12] A significant advantage of these techniques is the ability to distinguish between free or localized carriers, excitons, and surface plasmon resonances, since they have different signatures in the photoconductivity spectrum.[13] Another advantage is that the transport parameters such as mobility can be measured without the need of fabricating contacts thereby providing rapid feedback for optimisation and the use of NWs for applications in transistors and transparent conductive electrodes.[14,15]

In this work, we have utilized TDTS to investigate the optical properties and intrinsic conductivity of SnO_2 NWs in the THz region. Furthermore, TRTS measurements were used to probe the carrier dynamics and transport properties on ps timescale. Time resolved measurements revealed that Auger recombination is negligible for carrier densities smaller than 5×10^{18} carriers/cm^3. Furthermore, carrier density studies have determined a recombination time of 2.5 ns and an Auger coefficient of $\gamma = (7.2 \pm 2.0) \times 10^{-31}$ cm^6/s. The conductivity measurements reveal localization of carriers and strong suppression of long transport. From the intrinsic conductivity data, we have estimated a mobility of (72 ± 10) cm^2/Vs. Moreover an analysis of the photoconductivity measurements based on the Drude-Smith model revealed that the scattering time decreases from 140 to 70 fs as the carrier density increases from 0.5×10^{19} cm^{-3} to 5.5×10^{19} cm^{-3}.

A *Spectra Physics Tsunami* Ti:Sapphire oscillator and a *Spitfire* regenerative amplifier were used to generate output pulses of 100 fs at 800 nm, with a repetition rate at 1 kHz and energy of 1.1 mJ/pulse. These, pulses are introduced into a conventional TRTS experimental apparatus.[13] UV was used to excite carriers into the conduction band states since SnO_2 is a wide bandgap semiconductor. This was achieved via third harmonic frequency mixing, providing pump pulses at 266 nm and energy up to 70 μJ/pulse. The generation of THz pulses was accomplished by nonlinear optical rectification in a 0.5 mm $\langle 110 \rangle$ ZnTe nonlinear crystal, and detection was achieved via free-electrooptic sampling technique using a second 0.5 mm $\langle 110 \rangle$ ZnTe crystal.

SnO_2 NWs were grown on 1 nm Au/Si(001) using a low pressure chemical vapour deposition reactor at 800 °C under a flow of 600 sccms Ar: 10 sccms O_2 at 1×10^{-3} mbar for 1 h, described in detail elsewhere.[8] The SnO_2 NWs have diameters of 50-100 nm and lengths up to ≥ 10 μm. For the measurements the SnO_2 NWs were transferred on quartz substrate by drop casting after being harvested from the parent substrate by sonication.

Initially, the carrier dynamics of the SnO_2 NWs were measured by photoexciting at 266 nm and sampling the change in the peak of the THz transmission signal as a function of temporal delay between pump and probe pulses. Figure 1 shows the negative change in THz pulse transmission within a time window of 400 ps for different excitation carrier densities between 5×10^{18} cm^{-3} and 5.6×10^{19} cm^{-3}.

By comparing the normalized pump fluence-dependent transmission traces shown in the inset of the Fig. 1, it is obvious that carrier relaxation becomes progressively faster as the photogenerated carrier density increases. Such behaviour is expected when Auger recombination effects contribute to the carrier relaxation. To verify the validity of this

a)Electronic mail: othonos@ucy.ac.cy.

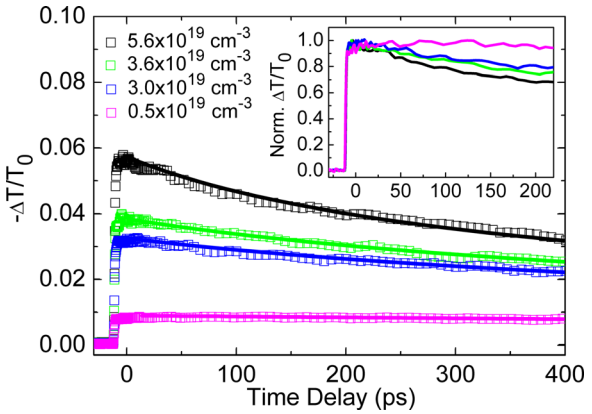

FIG. 1. Time resolved change in the THz transmission (dotted lines) using different pump fluences corresponding to carrier densities between $(0.5–5.6) \times 10^{19}\,\mathrm{cm}^{-3}$. For comparison purposes, the inset shows the normalized change in the transmission signal.

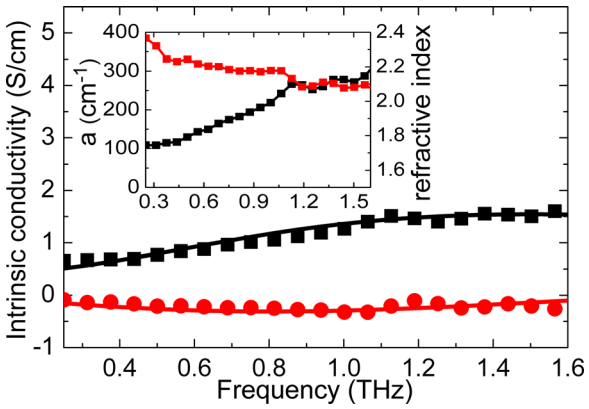

FIG. 2. Real (black squares) and imaginary (red circles) parts of the intrinsic conductivity in SnO_2 NWs for the region 0.25–1.6 THz. Solid lines have been obtained using the Drude–Smith model. The inset shows the frequency dependence of the refractive index (red squares) and absorption coefficient (black squares).

assertion, a differential rate equation model is used to explain the evolution of photogenerated carriers back to equilibrium. In this model, the recombination time is described by the first term of the differential equation whereas Auger recombination is described by the second term[16]

$$\frac{dN(t)}{dt} = -\frac{N(t)}{\tau} - \gamma \mathrm{N}^3(t), \tag{1}$$

where $N(t)$ corresponds to carrier density, τ is the recombination time and γ the Auger coefficient of SnO_2. The recombination time τ of the system was determined at the lowest carrier density where Auger recombination is considered negligible. Best fits were obtained when using a single exponential decay with a recombination time of $\tau = 2.5$ ns. The Auger coefficient γ in this NW system, was determined to be equal to $\gamma = (7.2 \pm 2.0) \times 10^{-31}\,\mathrm{cm}^6/\mathrm{s}$, which is in agreement with values reported in the same NWs elsewhere.[8]

TDTS measurements were utilized to determine the optical properties and the intrinsic conductivity of SnO_2 NWs in the THz region. Initially, measurements of the temporal THz electric field transmitted through SnO_2 NWs grown on Au/quartz without optical excitation, but also through plain quartz substrate were determined. The refractive index of the quartz substrate, was determined to be nearly constant ≈ 2.0 over the spectral region between 0.25-2 THz, while the absorption coefficient was considered negligible ($\leq 5\,\mathrm{cm}^{-1}$), in agreement with values reported elsewhere.[17] The properties of the SnO_2 NWs were extracted using the analysis followed for thin films.[18] No differences in the results were determined when an effective medium approximation (EMA) analysis was utilized.[19] The inset of Fig. 2 shows the refractive index (red squares) and absorption coefficient (black squares) calculated in the region of 0.25–1.6 THz. Clearly evident is a larger index of refraction than the refractive index of bulk SnO_2 in the visible region, $n \approx 2$,[20] which decreases monotonically from $\approx$2.4 to $\approx$2.1 with increasing THz frequency.

On the other hand, the absorption coefficient is monotonically increasing in the probed region from $110\,\mathrm{cm}^{-1}$ at 0.25 THz up to $300\,\mathrm{cm}^{-1}$ at 1.6 THz. Furthermore, Fig. 2 displays the real (black squares) and imaginary (red circles) parts of the frequency dependent intrinsic conductivity determined from the analysis of the data. Here we should point out that the real part of the conductivity increases monotonically, while the imaginary part of the conductivity appears to be negative. Similar behaviour has also been observed in Si nanocrystals,[10] InN nanorods,[21] and ZnO NWs,[11] which is described by the Drude–Smith model[22] and is attributed to the localization of carriers. This model, as described by Eq. (2), includes additional terms to modify the classical Drude system and incorporates the effect of incomplete randomization of carrier momentum after collisions

$$\sigma(\omega) = \frac{\mathrm{N}e^2\tau}{m^*(1 - i\omega\tau)}\left[1 + \sum_{j=1}^{\infty}\frac{c_j}{(1 - i\omega\tau)^j}\right], \tag{2}$$

where e is the electron charge, m^* the effective electron mass, τ the *scattering time*, and c_j the *persistence of velocity* after a number of j collisions. In the above equation we utilized the effective electron mass $m^* = 0.275\,m_0$ (m_0 the bare electron mass) for bulk SnO_2.[23] In practice, only the first term of the summation of Eq. (2) is taken into account. In an attempt to give a physical meaning to the *persistence of velocity* Monte Carlo simulations have been performed for the case of free charge carriers localized in semiconducting nanoparticles.[24] It was found that when the nanostructure dimensions are comparable to the mean free path, similar observations with that given by the Drude–Smith model can be expected, where the *persistence of velocity* c_1 is related to the possibility that carriers backscatter at the surface of the nanostructure. Clearly, the Drude–Smith model fits very well the experimental data shown in Fig. 2 as denoted by red and black lines for real and imaginary part of conductivity. The intrinsic carrier concentration in the SnO_2 NWs was determined to be $n = (3.3 \pm 0.4) \times 10^{16}\,\mathrm{cm}^{-3}$ whereas the scattering time τ (75 ± 7) fs. Furthermore, the persistence of velocity was estimated to be $c_1 = -0.85 \pm 0.02$. Given that the *persistence of velocity* is less than -0.5 this indicates suppression of long carrier transport due to the spatial localization of carriers. The estimated value of c_1 and scattering

time correspond to a macroscopic dc mobility of $\mu = \mu_m(1 + c_1) \approx (72 \pm 10)$ cm^2/Vs, where μ_m is the respective bulk mobility.

To further improve our understanding on the transport properties of the carriers in photoexcited SnO_2 NWs, photoconductivity measurements were performed. Here it is important to note that it is necessary to account for the filling factor of the NWs f_s on the substrate in order to obtain reliable values for the measured photoconductivity. Following careful examination of different SEM images the filling factor was estimated to be approximately 0.25. We should point out that a similar procedure has been previously applied for GaAs NWs (Ref. 12) in extracting the photoconductivity. In our measurements we utilized ultraviolet pulses at 266 nm at various pump energies in the range between 20.9–1.8 μJ/pulse. Measurements were carried out with the probe beam delayed at ~5 ps following the excitation pulse, where the THz signal has reached a maximum plateau, and before significant recombination of carriers could occur. We notice that the frequency dependence of the real part of the photoconductivity is similar to that obtained for the non-excited SnO_2 NWs, as seen in Fig. 3(a). On the other hand the imaginary part of the photoconductivity shown in Fig. 3(b) is more complex. It appears to be negative at low frequencies and becomes positive at larger frequencies. At first glance such behaviour can be explained by either the Drude–Smith model or by the surface plasmon resonance model[25] as has been proposed for GaAs NWs.[12] However, a careful estimate of the SnO_2 NWs plasmon frequency for the carrier densities considered in this work indicate that it is out of the frequency range measured here (>14 THz, when $N_0 = 0.5 \times 10^{19}$ carriers/cm^3) thus eliminating the plasmon resonance model. Moreover, the Drude–Smith model can sufficiently describe the experimental data as shown by the solid lines in the Figs.

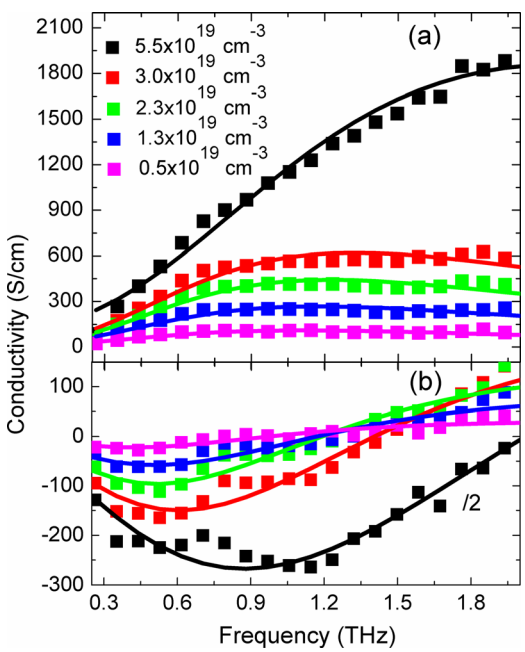

FIG. 3. (a) Real and (b) imaginary parts of conductivity spectrum of SnO_2 NWs (dot lines) at different pump energies corresponding to carrier densities $N_0 = (5.6–0.5) \times 10^{19}$ cm^{-3}, 5 ps after photoexcitation. Solid lines correspond to best fits using the Drude-Smith model.

3(a) and 3(b) corresponding to the best fits. Table I display the extracted best fitting parameters using the Drude-Smith conductivity for carrier density N, scattering time τ and *persistence of velocity* c_1 for the different pump energies utilized in this work.

From the Table I it appears that a larger fraction of the photo-generated carriers contribute to the photoconductivity with increasing pump fluence. This is to be expected given that, 5 ps after photoexcitation, most of the photogenerated carriers in the SnO_2 NWs lose their excess energy and relax to the bottom of the conduction band or move into shallow defect states or surface states. For such high pump fluences, we expect that these states are saturated by the photoexcited carriers in SnO_2 NWs as has been previously observed.[8] In addition to the fact that no band to band recombination of carriers is expected, since no band edge photoluminescence has been observed from these SnO_2 NWs, a large number of the initial carriers that are generated remain in conduction band states. These free charge carriers are likely to contribute to the photoconductivity. Therefore, in the case of the highest pump fluence it seems that the majority of photoinduced carriers contribute to the conductivity signal and the estimated carrier density ($\approx 4.5 \times 10^{19}$ carriers/cm^3) is close to the initial phogenerated carrier density ($\approx 5.5 \times 10^{19}$ carriers/cm^3). The difference is most likely due to the fact that some of the carriers become immobile as they are trapped into the defect/interface states. Accordingly, as the pump fluence decreases the number of initial carriers contributing to the photoconductivity becomes lower, since more carriers are trapped into defect/interface states. Furthermore, the *persistence of velocity* in this sample is strongly negative even for the lowest pump fluences used. This behavior suggests a strong localization of carriers in the SnO_2 NWs, since transport of carriers between different SnO_2 NWs is inhibited. There are several ways that carriers may transport into adjacent NWs, such as diffusion through pathways between connected NWs, tunneling or hopping.[26] As a consequence of the low volume filling factor of the SnO_2 NWs on the quartz substrate few interconnections between adjacent SnO_2 NWs exist. In addition the SnO_2 NWs are placed onto insulating SiO_2 and are surrounded by air so the potential barriers at the surface of the NWs are high, thereby preventing tunneling or hopping of carriers into different NWs. Moreover, the *persistence of velocity* becomes slightly more negative as the carrier density increases. We speculate that for such high carrier densities, a large number of carriers remain in the conduction band and a limited number of pathways exist for

TABLE I. Parameters of carrier density N, scattering time τ, and persistence of velocity c_1, extracted by fitting experimental data of Fig. 3 to Drude-Smith conductivity model.

$N_0 \times 10^{19}$ (carriers/cm^3)	$N \times 10^{19}$ (carriers/cm^3)	τ (fs)	C_1
5.5	4.5 ± 0.2	70 ± 4	-0.94 ± 0.01
3.0	0.9 ± 0.1	110 ± 5	-0.93 ± 0.01
2.3	0.5 ± 0.1	119 ± 4	-0.91 ± 0.01
1.3	0.40 ± 0.08	120 ± 6	-0.90 ± 0.01
0.5	0.15 ± 0.05	130 ± 6	-0.90 ± 0.01

carriers to move into a different SnO_2 NW, so carriers become localized. As expected the scattering time appears to be also carrier density dependent and becomes larger as the carrier density increases.

Results obtained from TDTS measurements cannot be directly compared to the results from the TRTS technique, since samples with different filling factor were used. In the case of the TDTS measurements, properties of SnO_2 NWs with a larger filling factor were investigated in contrast to those transferred. We believe that this is the reason for the slightly smaller negative value of persistence of velocity.

In summary, intensity dependent carrier dynamics have been measured and the time dependence of the photogenerated carriers modelled by including Auger recombination in a rate equation. This gave an Auger coefficient $\gamma = (7.2 \pm 2.0) \times 10^{-31}\,cm^6/s$ and a recombination time of 2.5 ns. We demonstrate that the intrinsic conductivity and photo-conductivity is affected by carrier localization in the SnO_2 NWs, which is a result of the diameter and low density of SnO_2 NWs on the substrate. For carrier densities between $0.5–5.5 \times 10^{19}\,cm^{-3}$, we find that the scattering time decreases from 140 to 70 fs. The refractive index varies between 2.4-2.1 in the probed region, while the mobility of SnO_2 NWs was found to be $(72 \pm 10)\,cm^2/Vs$.

[1]J. Maier and W. Gopel, J. Solid State Chem. **72**, 293 (1988).
[2]S. A. Pianaro, P. R. Bueno, E. Longo, and J. A. Varela, J. Mater. Sci. Lett. **14**, 692 (1995).
[3]N. Amin, T. Isaka, A. Yamada, and M. Konagai, Sol. Energy Mater. Sol. Cells **67**, 195 (2001).
[4]N. Yamazoe, Sens. Actuators B **5**, 7 (1991).
[5]Z. W. Pan, Z. R. Dai, and Z. L.Wang, Science **291**, 1947 (2001).
[6]Z. Liu, D. Zhang, S. Han, C. Li, T. Tang, W. Jin, X. Liu, B. Lei, and C. Zhou, Adv. Mater. **15**, 1754 (2003).
[7]M. J. Zheng, G. H. Li, X. Y. Zhang, S. Y. Huang, Y. Lei, and L. D. Zhang, Chem. Mater. **13**, 3859 (2001).
[8]A. Othonos, M. Zervos, and D. Tsokkou, Nanoscale Res. Lett. **4**, 828 (2009).
[9]M. C. Beard, G. M. Turner, J. E. Murhpy, O. I. Micic, M. C. Hanna, A. J. Nozik, and C. A. Schmuttenmaer, Nano Lett. **3**, 1695 (2003).
[10]D. G. Cooke, A. N. MacDonald, A. Hryciw, J. Wang, Q. Li, A. Meldrum, and F. A. Hegmann, Phys. Rev. B **73**, 193311 (2006).
[11]J. B. Baxter and C. A. Schmuttenmaer, J. Phys. Chem. **110**, 25229 (2006).
[12]P. Parkinson, J. Lloyd-Hughes, Q. Gao, H. H. Tan, C. Jagadish, M. B. Johnston, and L. M. Herz, Nano Lett. **7**, 2162 (2007).
[13]R. Ulbricht, E. Hendry, J. Shan, T. F. Heinz, and M. Bonn, Rev. Mod. Phys. **83**, 543 (2011).
[14]Q. Wan, E. Dattoli, and W. Lu, Small **4**, 451 (2008).
[15]Y.-D. Ko, J.-G. Kang, J.-G. Park, S. Lee, and D.-W. Kim, Nanotechnology **20**, 455701 (2009).
[16]M. Ghanassi, M. C. Schanne-Klein, F. Hache, A. I. Ekimov, D. Ricard, and C. Flytzanis, Appl. Phys. Lett. **62**, 78 (1993).
[17]D. Grischkowsky, S. Keiding, M. V. Exter, and C. Fattinger, J. Opt. Soc. Am. B **7**, 2006 (1990).
[18]T.-R. Tsai, S.-J. Chen, C.-F. Chang, S.-H. Hsu, T.-Y. Lin, and C.-C. Chi, Opt. Express **14**, 4898 (2006).
[19]F. J. García-Vital, J. M. Pitarke, and J. B. Pendry, Phys. Rev. Lett. **78**, 4289 (1997).
[20]E. Shanthi, V. Dutta, A. Banerjee, and K. L. Chopra, J. Appl. Phys. **51**, 6243 (1980).
[21]H. Ahn, Y.-P. Ku, Y.-C. Wang, C.-H. Chuang, S. Gwo, and C.-L. Pan, Appl. Phys. Lett. **91**, 163105 (2007).
[22]N. V. Smith, Phys. Rev. B **64**, 155106 (2001).
[23]K. J. Button, C. G. Fonstad, and W. Dreybrodt, Phys. Rev. B **4**, 4539 (1971).
[24]H. Němec, P. Kužel, and V. Sundström, Phys. Rev. B **79**, 115309 (2009).
[25]J. M. Pitarke, V. M. Silkin, E. V. Chulkov, and P. M. Echenique, Rep. Prog. Phys. **70**, 1 (2007).
[26]L. V. Titova, T. L. Cocker, D. G. Cooke, X. Wang, A. Meldrum, and F. A. Hegmann, Phys. Rev. B **83**, 085403 (2011).